

Received 16 March 2023, accepted 1 April 2023, date of publication 7 April 2023, date of current version 24 April 2023.

Digital Object Identifier 10.1109/ACCESS.2023.3265572

RESEARCH ARTICLE

Non-Gaussian Traffic Modeling for Multicore Architecture Using Wavelet Based Rosenblatt Process

AMIT CHAURASIA¹, (Member, IEEE), VIJAY SHANKAR SHARMA¹, (Member, IEEE),
CHIRANJI LAL CHOWDHARY², SHAKILA BASHEER³,
AND THIPPA REDDY GADEKALLU^{2,4,5}, (Senior Member, IEEE)

¹Department of Computer and Communication Engineering, Manipal University Jaipur, Jaipur, Rajasthan 302007, India

²Department of Software and Systems Engineering, Vellore Institute of Technology, Vellore, Tamil Nadu 632014, India

³Department of Information Systems, College of Computer and Information Science, Princess Nourah bint Abdulrahman University, P.O. Box 84428, Riyadh 11671, Saudi Arabia

⁴Department of Electrical and Computer Engineering, Lebanese American University, Byblos 1526, Lebanon

⁵Zhongda Group, Baibu, Haiyan, Jiaxing, Zhejiang 314312, China

Corresponding author: Chiranji Lal Chowdhary (chiranji.lal@vit.ac.in)

This research is supported by Princess Nourah bint Abdulrahman University Researchers Supporting Project number (PNURSP2023R195) Princess Nourah bint Abdulrahman University, Riyadh, Saudi Arabia.

ABSTRACT Networks-on-Chip (NoCs) provides a packet-based communication model for the System-on-Chip (SoC) architecture to achieve objectives of lower power, higher performance and optimized area. To evaluate NoC performance and explore architectural design options, synthetic traffic models provide better solution in terms of simulation flexibility and faster simulation. In this synthetic traffic, models are generated for the simulation to optimize the computational resources requirements which will be placed inside NoC's architecture before the early design process. In this paper, Wavelet-based Rosenblatt synthetic traffic [RST] is designed and examined which is a non-Gaussian process based on the 2nd-order Hermite Process. The proposed traffic is applied to SPLASH-2 benchmarks and compared with Gaussian and Non-Gaussian traffic on the parameters of latency, power and buffer-loss. We applied the synthetic traffic on multicore architecture to capture parameters which would be helpful for network designers to choose optimized network resources during the early design architecture. We demonstrate our traffic model: first, how it can be used to describe and acquire non-gaussian burstier traffic on NoC; second, how it can be used to produce synthetic traffic traces that can drive exploration of the early design space for NoCs. Our traffic model helps the chip network designer to choose optimized queue storage inside the router in early design process.

INDEX TERMS Networks-on-chip, Rosenblatt process, self-similar process, traffic modelling.

I. INTRODUCTION

The networks are becoming more and more complex and in this era of ubiquitous computation where every gadget is equipped with small processing units, with more computation capabilities and the need for less space. As the different high-definition images or sequences of images make this computation architecture busier. The number of cores is increasing in the computation devices, to streamline the processing capabilities for a huge volume of data.

The associate editor coordinating the review of this manuscript and approving it for publication was Maurizio Casoni¹.

This multicore architecture requires functional balancing to achieve parallelism in the processing chips and communication between chips using networking. In the early design of the on-chip architecture, the computational resources requirement becomes a bottleneck, so to make efficient architecture, it requires synthetic traffic to capture the real behaviour. The real-time traffics are not flexible enough to capture the real nature and causes the simulation time to range from hours to days.

The problem with bus-based communication is network utilization, as it suffers from problems such as high latency, deadlock, channel allocation, and flits dropping. As the size

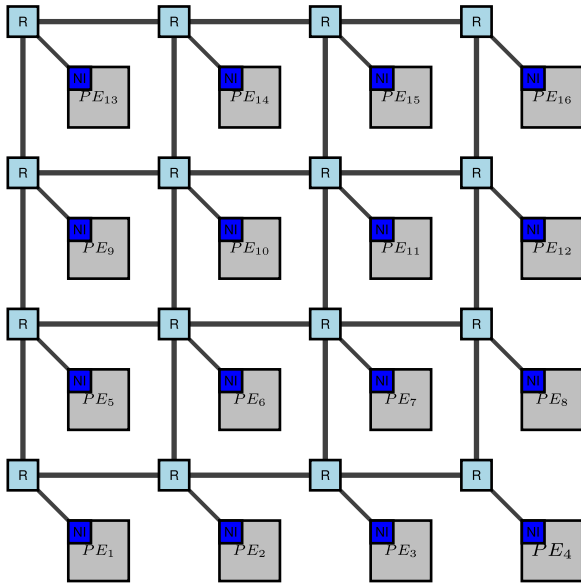


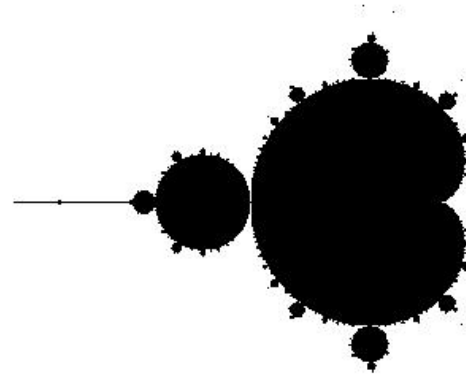
FIGURE 1. 4 × 4 Mesh Architecture with PE's and routers connected by network interface.

of buffers is limited in the architecture of micro routers, it is hard for network designers to choose the best sizes for the buffers inside the router. The concept of multiple IPs (intellectual property) in FIGURE 1 placed inside the chip system necessitates communication between each tile. The router is placed as the interface with each tile, which helps in the communication between different cores. As in the early design, it is hard and complicated to predict the optimal sizes of the storage queues with real-time traffic. Because of this, the simulation on flits in the micro router architecture needs flexibility and less simulation time traffic. Synthetic traffic is required because it is flexible and saves a lot of simulation hours.

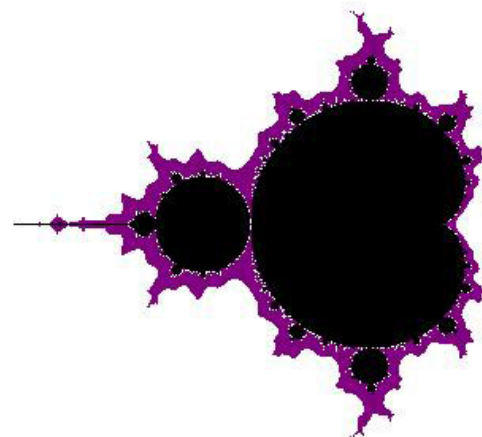
The realistic traffics are often suffers from process mapping optimizations and the traffics are not resilient with the higher failure rates due to the network routing algorithms. The other limitations with the realistic traffic simulation are the duration of simulation and the requirement of realistic hardware. In [1] the realistic traffic models are simulated for the mixed-torus architecture and the traffic is mainly loaded in the centre of architecture and non uniformly loaded traffics are not analyzed. In the [2] used both the realistic traffic and synthetic traffic patterns to analyze the threat of hardware trojans in the routing process and reduces the average network latency by 38% in realistic traffic and 48% in synthetic traffic patterns. It has also reduces the deflected average latency by 97% for synthetic traffic and 62% for realistic traffics.

A. MOTIVATION AND SCOPE

According to the arbitration result, the on-chip bus permits only one communication transaction at a time; hence, the average communication bandwidth of each processing element is inversely proportional to the total number of IP cores



(a) Simple Fractal



(b) Coloured Fractal

FIGURE 2. Self-similar fractals.

in a system. In modern MP-SoC (multiprocessor system-on-chip) and CMP (chip multiprocessor) designs, a bus-based architecture is intrinsically not scalable for large systems due to this characteristic. This scaling limitation may be lifted by implementing numerous on-chip buses in a hierarchical architecture or in a segregated way, however this calls for application-specific grouping of processing units and construction of alternative communication protocols.

The emerging MP-SoC and CMP architectures require high throughput, low latency, and reliable global communication services, which are not met by the current dedicated bus-based on-chip communication infrastructure due to the increased density of processors and cores made possible by advances in semiconductor fabrication technology. There are

potential challenges with timing closure, performance, and scalability when attempting to implement such concepts in a bus architecture. To be more specific, the feature size of current silicon devices is shrinking below 50 nm, which causes global connectivity delays to limit the maximum possible processing speed.

The self-similarity property, it has various applications in the field of hydrology [3], turbulence [4], stock market and finance [5], [6], [7], statistical inference [8], [9] and internet [10]. A self-similar object which repeats either exactly or approximately to itself in finer and finer details. In Figs. 2a and 2b are representing the self-similar properties in finer detail as we enlarge the image. The notion of self-similarity is used to design synthetic traffic for multimedia applications. In this literature, the internet aspect is used to generate the synthetic traffic for multicore architecture simulation. It has three aspects of study one is the spectrum, the second is the finite integration and the third is the wavelet representation.

In gaussian synthetic traffic [GST] [11] is generated for the raw video using the Hurst parameter (H) [12] which captures the feature of long-range dependency [13] of the process i.e. how bursty the data would be, but the traffics produced are Gaussian in nature, while the study shows that non-Gaussian synthetic traffic [NGST] processes are better models to capture real-time characteristics to capture burstiness [14], [15]. In [16] traffics are generated for long- and short-range dependent processes and model a multi-fractal non-stationary process to estimate the average-case and worst-case scenario for latency models. In [17] mathematical models are designed for the performance analysis of DCoC (data centres on-chip) relying on the multi-fractal dynamics. The basis for generating synthetic traffic is taken from the concept of self-similarity. In FIGURE 2 [18] we can see the various objects are broken into parts that are of the same shape but the size is reduced, this will be the basis for traffic generation using the self-similar properties.

B. OVERVIEW OF ROSENBLATT PROCESS

Leland et. al. demonstrated self-similarity of network traffic in 1993 [19] by noting that a rapid increase in network stream was not in sync with the evolution of a time unit. The Hurst parameter, a measure of the degree to which network traffic exhibits self-similarity. The Hurst parameter is unique in its ability to define the degree of self-similarity and abruptness in Network traffic. It is possible to assess whether or not the usual, real-time data stream from the network is compatible with the statistical self-similarity and the LRD properties of network traffic by looking at the value of the Hurst parameter. The calculation of the Hurst parameter, which is central to the field of network traffic modelling [20], is based on a number of factors, including the rate at which packets are lost in transit and the likelihood of congestion. Therefore, it is crucial for network management and control, as well as for self-similar traffic modelling and control, to estimate the

Algorithm 1 Algorithm for Generating Fractional-Rosenblatt Motion Process Using CIET (Circular Embedding Technique)

- 1: Choose a parameter $U \in (0.25, 0.5)$ defining FRMP.
 - 2: Choose the multi-resolution orthogonal wavelet basis, which has zero-moments N .
 - 3: The length of time for the FRMP $T = 2N$. Selecting the Scale 2^{-l}
 - 4: **procedure** Initial_FARIMA(N, I, fbm)
 - 5: Choose the value of L such that $-N \geq L \geq I$
 - 6: Choose the low and high-pass fractional filter δ^d and θ^d , because r is limitless, these filters must be truncated at r .
 - 7: **for** $j \leftarrow 0$ to $r + 2^{(N+L)}$ **do**
 - 8: $\Lambda^d = CIET(fbM)$
 - 9: **end for**
 - 10: **for** $j \leftarrow 0$ to $I - L$ **do**
 - 11: $\Lambda^{(v)} = FFT(\Lambda^d)$
 - 12: **end for**
 - 13: **for** $i \leftarrow 0$ to $2^{(N+L)}$ **do**
 - 14: $\tilde{Q}_{v,0}^{(k,2)} = \sum_{0 \geq i \geq k} \left((\Lambda^{(v)})^2 - \mathbb{E}(\Lambda^{(v)})^2 \right)$
 - 15: **end for**
 - 16: Using the following equation, generate the sequence using an estimate of FRMP.
- $$Y_{k,2} \left(L, I, t = v^{2^{-l}} \right) = P_k 2^{-2kl} \tilde{Q}_{v,0}^{(k,2)} \quad (1)$$
- where $P_k = \frac{\Gamma(k)\Gamma(1-k)\sqrt{4(k-1)k}}{\Gamma(1-2k)}$
- 17: return $Y_{k,2}$ in vector.
 - 18: **end procedure**

Hurst parameter based on the monitoring data of traffic in a particular time period.

In [21], observed long-range correlation in LAN traffic, providing proof for the presence of power law connections in network traffic. This opened up the subject of network traffic and performance research to the idea of self-similarity, and its related notion, long-range dependency (LRD). Before this discovery, models like Poisson processes, which presume that traffic displays no long-term association, were the backbone of studies of network traffic and performance. Queueing performance in networks with long-term correlations may differ significantly from that in networks with traffic that is expected to be totally uncorrelated or with relatively modest correlations over short time periods.

In [3] stated the Rosenblatt process is a self-similar non-Gaussian process. Rosenblatt process has the same covariance as the fractional Brownian motion (fBm). The Rosenblatt process is also used for the estimation of the Hurst index by deriving the exact equations based on limiting distributions. For the time-series process the Hurst index (H) is used to measure the long-range dependency by comparing the autocorrelations for the time-series process and measuring the rate at which it decreases between the lags.

The inter-arrival packets time is considered a time-series process. Earlier, the Hurst index is used in hydrology for the construction of a dam on the Nile river to measure the rain and drought conditions for a long period [22].

It has been discovered that fBm is the only continuous Gaussian process that is capable of producing self-similar increments while remaining stationary. The qualities listed above for $H > 0.5$ i.e. which entails, the long-memory property and in many instances the Holder-continuity are shared by many more stochastic processes than only those with a Gaussian character. The Gaussian assumption may be unrealistic in certain scenarios, necessitating the adoption of an alternative self-similar process with stable increments. Hermite processes are a natural choice since they are an example of a non-Gaussian stochastic process that shows up as a limit in the so-called “Non-Central Limit Theorem.”

In Section II discussed the related work in the field of multicore architecture and traffic modelling using stochastic processes. This section discussed the ways to the estimation of Hurst index. In Section III algorithm is discussed for generating the non-Gaussian-based Rosenblatt Synthetic traffic. The algorithm used the Circular Embedding Technique for the generation of synthetic traffic. In Section IV findings are compared with the non-Gaussian-based traffic and Gaussian-based traffic with the help of end-to-end latencies, buffer-loss probability and energy dissipation using different traffic patterns. Finally, in Section V the article is concluded with outcomes of the findings of results and the future role of Synthetic traffic in multicore architecture.

II. RELATED WORKS

A stationary process having Gaussian sequence $(\varphi_j)_{j \in Y}$ with uni-variance and mean equal to zero with its correlation function $S(n) = \mathbb{E}(\varphi_0 \varphi_j) = j^{\frac{2H-2}{k}} C(j)$, with $H \in (0.5, 1)$ and C is a changing function that approaches infinity extremely slowly. Let k be the Hermite rank of the process, and L be the function defined as

$$L(e) = \sum_{a \geq 0} q_a U_a(e), \quad q_a = \frac{1}{a!} \mathbb{E}(f(\varphi_0) U_a(\varphi_0)), \quad (2)$$

where $U_a(e)$ is the Hermite degree polynomial with variable details a and $k = \min\{a | q_a \neq 0\} \geq 1$.

The polynomial of Hermite is defined as $U_a(e) = (-1)^a e^{\frac{x^2}{2}} \frac{d^a}{dx^a} e^{-\frac{x^2}{2}}$. The Non-Central Limit Theorem states that, $\frac{1}{n^H} \sum_{a=1}^{[j^H]} f(\varphi_a)$ in the context of finite-dimensional distributions, converges as $n \rightarrow \infty$ to the process in eq. (3). The Rosenblatt process is an example of a non-Gaussian process that with fixed increments is self-similar. The Rosenblatt process’s covariance functions are comparable in the sense that fBm is a self-similar process, but they differ in their core Gaussian. The method of Rosenblatt is important because it is an instance of Hermite Processes, which are the normalization of the sum of long-range dependent random variables. Simplest Hermite Processes is the fBm based

Rosenblatt process $Z_k(t)$ represented as

$$Y_U^k(t) = q(U, k) \int_{R^k} \left\{ \int_0^t \left(\prod_{a=1}^k (s - \xi_a)_+^{-\left(\frac{1}{2} + \frac{1-U}{k}\right)} \right) ds \right\} \times dB(\xi_1) dB(\xi_2) \quad (3)$$

where $\mathbb{E}(Y_k(1)^2) = 1$, makes $q(U, k)$ a normalized constant > 0 , $e_+ = \max(e, 0)$ for $e \in R$, whereas $B(\varphi)$ it is a standard Brownian motion, \int_{R^2} is the order k double Wiener-It’o multiple integrals. It is defined by $k \in (0.25, 0.50)$ called as *fractional Rosenblatt motion* (fRm) since it has a set increment.

The variable k is used to describe the processes in the eq. (3) and is referred to as the U . It’s calculated using a variety of methods described in [11] and [30]. The Y_k is expressed by the following equation in terms of the self-similarity index or Hurst parameter.

$$\{Y_k(qk)\}_{t \in R} \stackrel{d}{=} \{q^{2k} Y_k(t)\}_{t \in R} \quad (4)$$

The example may very well be found in Chapter 7 of [31], where $q \geq 0$ and the “ $\stackrel{d}{=}$ ” equality is based on a finite-dimensional distribution. The process distribution fRm tails are substantially heavier than those of the Gaussian distribution. Although both have stable increments, fRm has finite moments, which distinguishes it from fBm . In nature, fBm is Gaussian, whereas fRm is non-Gaussian. Rosenblatt describes the Rosenblatt process in [32], and more research may be found in [33] and [34]. In eq. (3), the Rosenblatt process is a double Wiener-It’o integral that may be generalised. It is a basic Hermite process known as Fractional Brownian Motion (fBm) if it is a single integral, and an order of 2^{nd} Hermite process known as Fractional Rosenblatt Motion (fRm) if it is a double integral. In [35] introduced the effect of low latencies and high throughput along with power consumption and optimized cost of running the traffic on multicore architectures. In the paper [36] author has represented the queuing traffic model based on G/D/1 model which provides the speed up of simulation 13 times. In [37] introduced the open feed-forward queuing model for the speed up of the simulation.

The performance of the Gaussian and Non-gaussian synthetic traffic is shown in the [38] where it is shown that the non-gaussian traffics are burstier than Gaussian traffic and they are the better model for generating burstier data. There are wavelet-based models also mentioned in the [39] for the synthetic traffic generation and the limitation with this model is that have the Gaussian distribution attribute to the synthetic traffic. For the accurate requirement of the non-gaussian model, the Hermite process is considered as the base which is non-gaussian in nature and it is the simplest non-gaussian Hermite process [40].

III. PROPOSED METHODOLOGY

The FARIMA (Fractionally Differenced Autoregressive Integrated Moving Average) wavelet processes, employs the Hurst index H for the starting phase of the process, for the

TABLE 1. Comparison of different traffic and routing approaches.

Ref.	Traffic Technique	Experimental Setup	Benchmarks	Optimization
[23]	Elevator-First Algorithm	3D mesh architecture	Traffic patterns (Uniform & Hotspot traffic)	Improves the performance in latency as the size of the network increases.
[24]	Dynamic XY Algorithm	NIRGAM 2.1	Generic Routing Algorithm	Achieves less packet loss
[25]	Application Pattern driven routing approach	NOXIM	VOPD, pip, etc.	Improvement of energy consumption and throughput
[26]	Congestion Aware Negative First routing algorithm with Fair Arbitration	Cycle accurate simulator	Congestion Aware Odd-Even routing (CAOE)	Improvement in the performance in throughput and latencies when compared with CAOE
[27]	Augmented virtual channel to reuse trace buffers to augment router buffers	BookSim	PARSEC, SPLASH2	Reduces the average packet latency and area of the router
[28]	Modelling of a Networks-on-Chip (NoC) using a communicating finite state machine (CFSM)	BookSim	Different routing Algorithms	Allows verification of various NoC features, such as starvation, livelock, etc., for any realistic traffic patterns for a given routing algorithm.
[29]	Bursty traffic based analytical models for priority-aware NoC	GEM5 2006 & 2017	SPEC CPU	Reduces 10% modelling error for cycle accurate NoC for mesh architecture

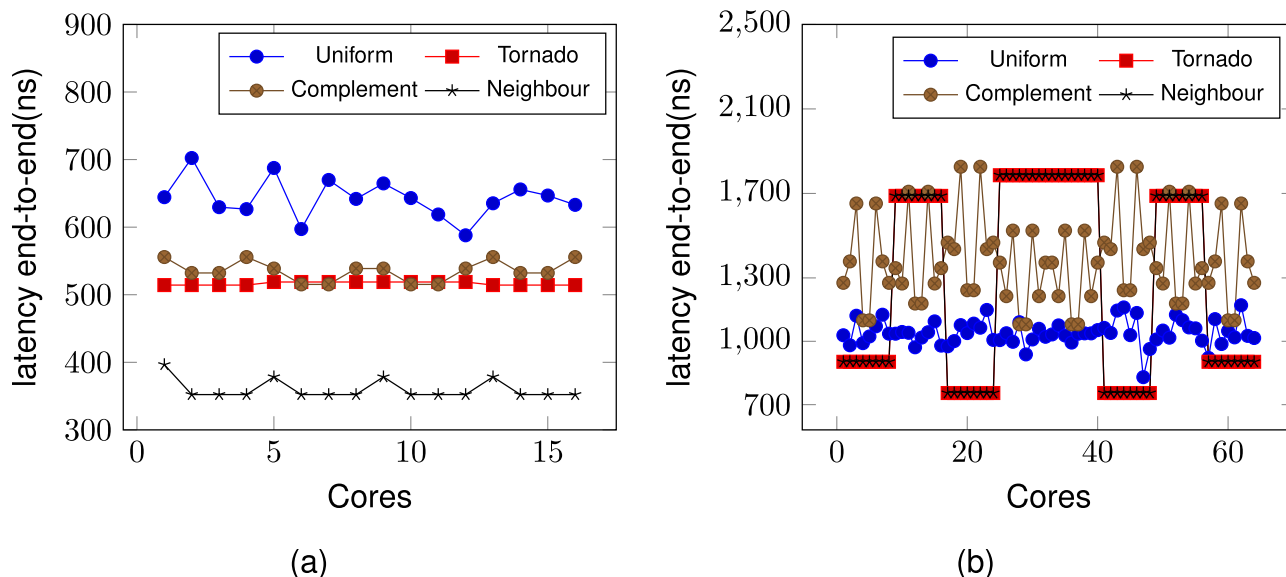


FIGURE 3. Average latency end-to-end(ns) for (a) 4 x 4 (b) 8 x 8 Mesh Interconnection Network for Tornado, Neighbour, Complement & Uniform traffic.

generation of the synthetic Rosenblatt process. The FARIMA processes are time series models generalized from ARIMA (Autoregressive Integrated Moving Average) models. The FARIMA processes are useful in modelling long-memory processes. In time series creation, the count of zero moments in the orthogonal multi-resolution analysis is crucial. A *fRm* approximation is used in the generation. The length

associated with truncated filters with N vanishing moments is represented in Table 1 in the article [39].

For the generation of the fractional filter, the filters are initialized as δ^0 and θ^0 which can be found from [41] page no. 196. The fractional filters are computed using the $\delta^g(z) = f^{(N+v)}\delta^0(z)$ as the order N increases $f^{(N+v)}$ the $h^{(v-N)}$ filters start to decay at a faster rate than usual $\delta^v(z)$ and $\theta^v(z)$.

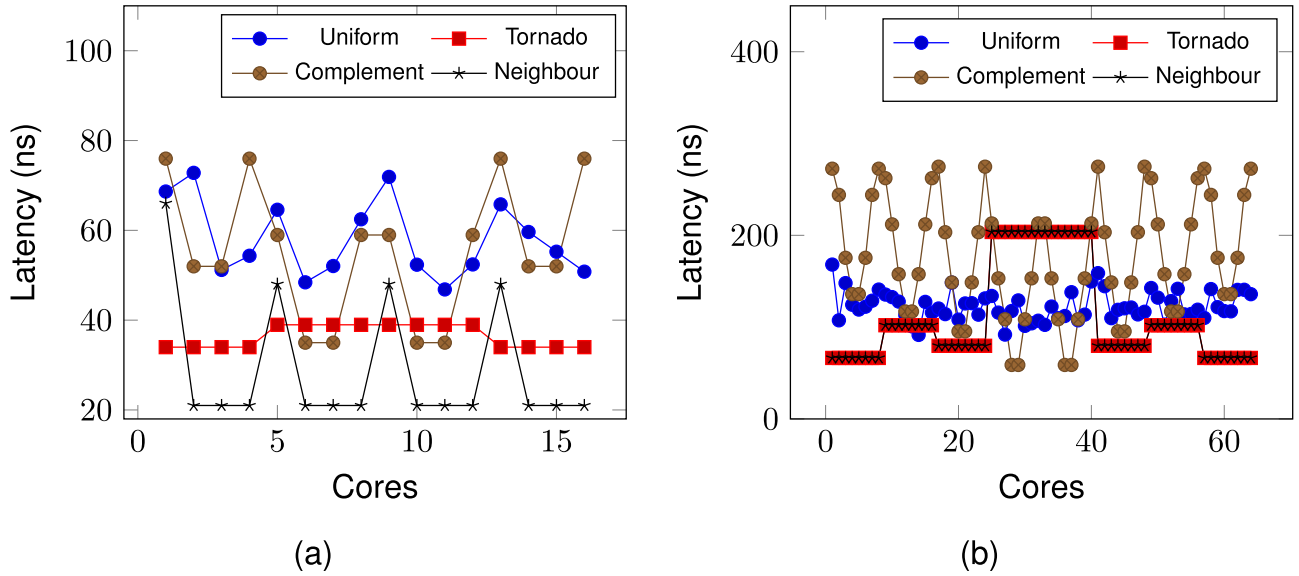


FIGURE 4. Network average latency(ns) for (a) 4×4 (b) 8×8 Mesh Interconnection Network for Tornado, Neighbour, Complement & Uniform traffic.

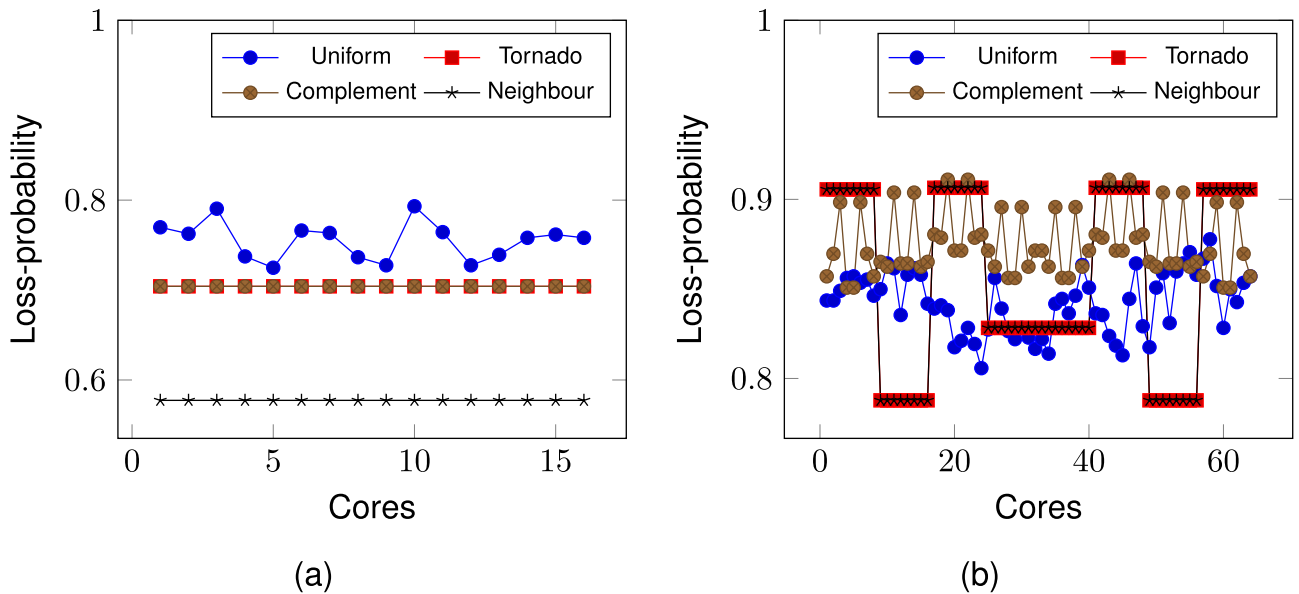


FIGURE 5. Loss probability (averaged) for (a) 4×4 (b) 8×8 Mesh topology for Tornado, Neighbour, Complement & Uniform traffic.

The fRm is generated using the algorithm, which is explained in 4 steps as follows:

- **Step 1:** collects the parameters utilized for the initial_FARIMA processes, including the U , 0-moments of multi-resolution orthogonal wavelet basis, process length (T), and a scaling parameter (T). Another parameter, L , was utilised, which ranges between $-N$ and I . N represents time length or multi-resolution wavelet basis with N zero moments for Fractional-Rosenblatt Motion Process (FRMP) such that $T = 2N$, and I is the scaling factor represented as 2^{-I} . The value of L is chosen from the range $[-N, I]$.

- **Step 2:** The starting filters are low and high-pass filters were selected. The range associated with these filters are infinite and must be trimmed.
- **Step 3:** In the following phase, the Circular Embedding Technique (CIET) is used recursively on the fBm which is passed as an argument in the function Initial_FARIMA. The CIET algorithm is utilised for process generation in [42] the usage of the CIET algorithm makes process generation faster than the FAST approximation approach. The Fast Fourier transform (FFT) is applied to the process created in the preceding substep, which is referred to as $\Lambda^{(v)}$. The use of FFT removes

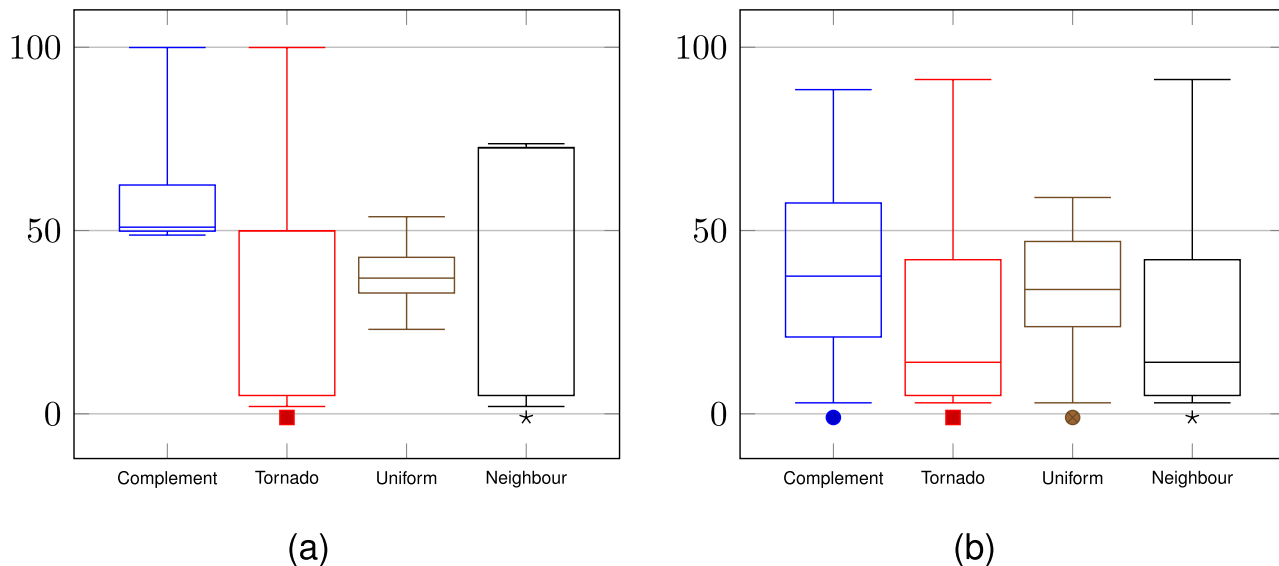


FIGURE 6. Average Link Utilization(%) boxplot for (a) 4 × 4 (b) 8 × 8 Mesh topology for Neighbour, Complement, Tornado & Uniform traffic.

the temporal information from the wavelet based data, as it may contains many fluctuations.

- **Step 4:** The partial sum of $\Lambda^{(v)}$ is created in the final sub-step of Step 3, eventually creating the initial_FARIMA process called *fRm*. In final step, the *fRm* approximation is used with eq. (1). In this step gamma function (Γ) is used as a function for the calculation of normalizing constant.

$$\Gamma(y) = \int_0^\infty x^{y-1} e^{-x} dx \quad (5)$$

The eq. (5) can be proved that gamma function is the factorial of non-negative integers which can also be represented as $\Gamma(n) = (n - 1)!$. The number of possible configurations of n is a concept made possible by the gamma function.

IV. RESULTS

We utilised the OMNeT++ simulator [43] for the simulation of synthetic traffic, and we built two interconnection network architectures for a mesh network with sizes of 4 × 4 and 8 × 8. The algorithm’s traffic is simulated to mimic traffic on the 2 mesh interconnection networks. The parameters used for the simulation in OMNeT++ are shown in TABLE 2. The simulation duration is of 2μs and the message length is of 4 packets and each packet has 8 flits where each flit is of 4 bytes. The XY routing algorithm is used for switching the flits from one core to another.

For the source & destination pair, we employed four traffic patterns: *complement*, *neighbour*, *tornado*, and *uniform*. The source is represented by x_i and the destination is represented by y_i in eqs. 6, 7, 8 and 9 respectively and n is total number of cores. The complement traffic chooses the destination based on the complement of the source address, which is calculated by subtracting the source from n shown in eq. (9). In the

neighbour, the destination is chosen by adding 1 to the source address represented in eq. (7). In the uniform traffic in eq. (6) destination is chosen by function *int_uniform*, which selects the value ranges from [1, n] with uniform distribution. In the tornado traffic in eq. (8) the source is added with half of the network size.

End-to-end and network latency are depicted in FIGURES 3 and 4, where the range of latencies varies from source to destination and hop-to-hop. The probability of packet-loss is displayed in FIGURE 5 for 8 × 8 and 4 × 4 mesh network, the average packet-loss for 8 × 8 when compared to 4 × 4 networks is higher as the higher order architectures have more probability for packet loss. The reason for this is the amount of traffic increases as the size of the architecture increases. The RST is compared to seven traces from the SPLASH-2 benchmark suite [44] using NGST and GST traffics. When compared to NGST, the synthetic traffic created for the Rosenblatt process achieved a higher latency of 6.64 %, but the latency is greater by 12.76 % than GST traffic.

$$y_i = (x_i + \text{int_uniform}(1, n)) \text{ mod } n \quad (6)$$

$$y_i = (x_i + 1) \text{ mod } n \quad (7)$$

$$y_i = (x_i + \frac{n}{2}) \text{ mod } n \quad (8)$$

$$y_i = (n - x_i) \text{ mod } n \quad (9)$$

The usage pattern of NoC channel bandwidth consumption is shown in FIGURE 6 representing link-utilization of four traffic patterns. For both designs, complement traffic has the highest link usage compared to other traffic patterns, whereas uniform traffic has the lowest. For the basic Hermite process and the Fractional Rosenblatt process, the energy dissipation by each tile in a 4 × 4 mesh network is depicted in FIGURE 7. While the fractional rosenblatt process is a burstier process, the simple hermite process has a lower power dissipation

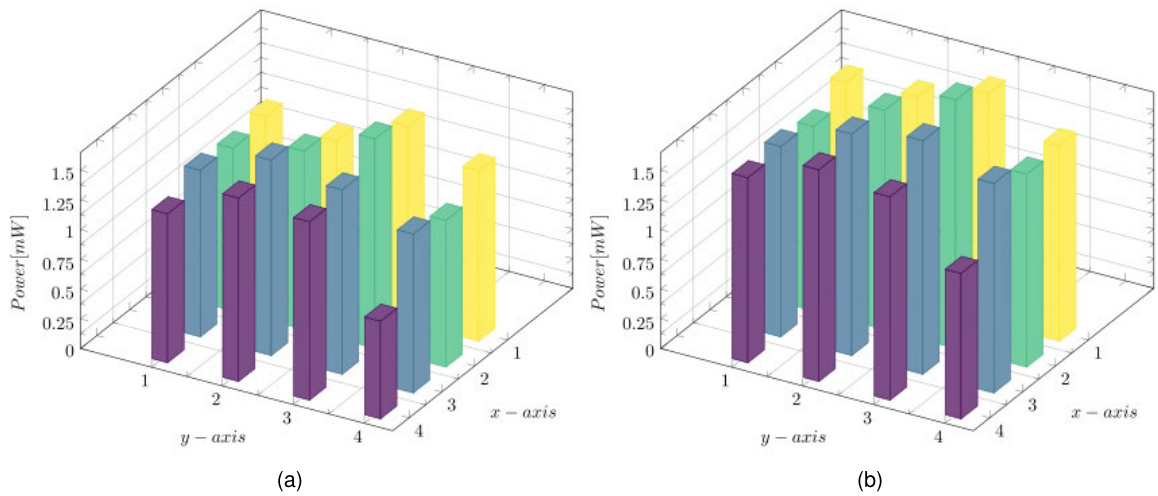


FIGURE 7. Power analysis for each tile of 4 × 4 Mesh network (a) Simple Hermite process (b) Fractional Rosenblatt process.

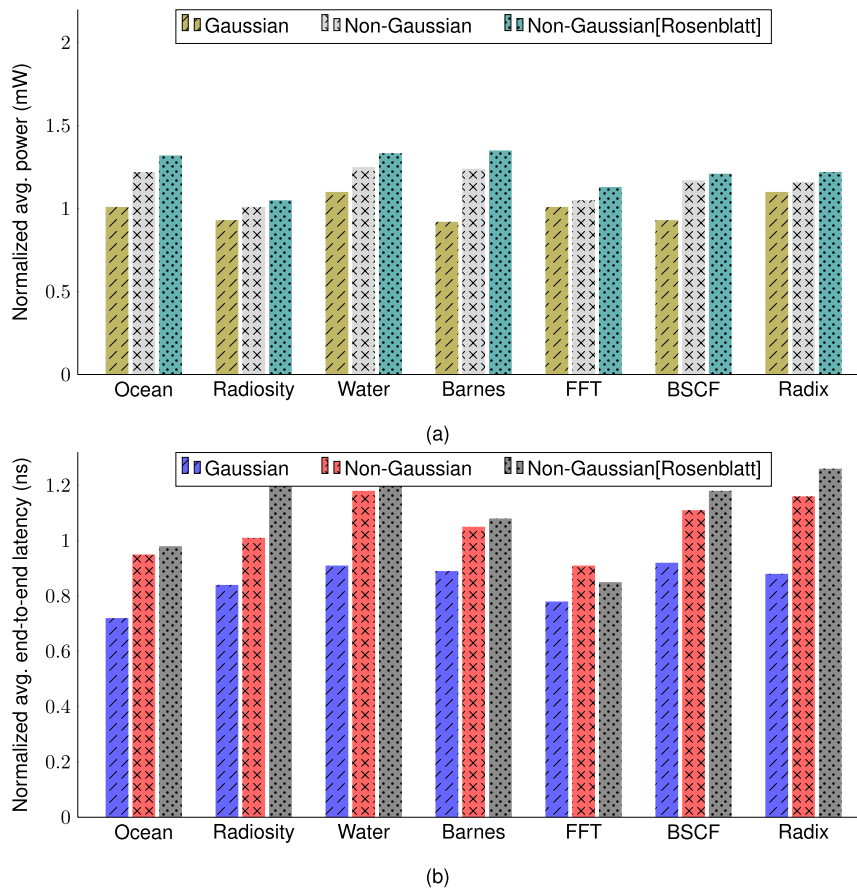


FIGURE 8. (a) Power (nW) and (b) Average end-to-end latency (ns) for SPLASH-2 Benchmark.

when compared to the fractional rosenblatt process. This is owing to the fact that the simple hermite process is more stable. All four traffic patterns in FIGURE 9 exhibit an average end-to-end latency for GST, NGST, and RST processes, indicating that RST processes are burstier than GST and NGST processes. The consistency of the GST, NST procedures causes the flow of packets to be slower than that of the RST because it results in an inaccurate perception of the ideal

communication resources requirement throughout the design process.

The average network latencies for all four traffic patterns are displayed in FIGURE 3, taking into account the three procedures of NGST, GST, and RST. In all four situations, the Rosenblatt process has a higher delay than Gaussian and non-Gaussian processes. Average latency (Average end-to-end latency (ns)) & packet-loss probability for GST,

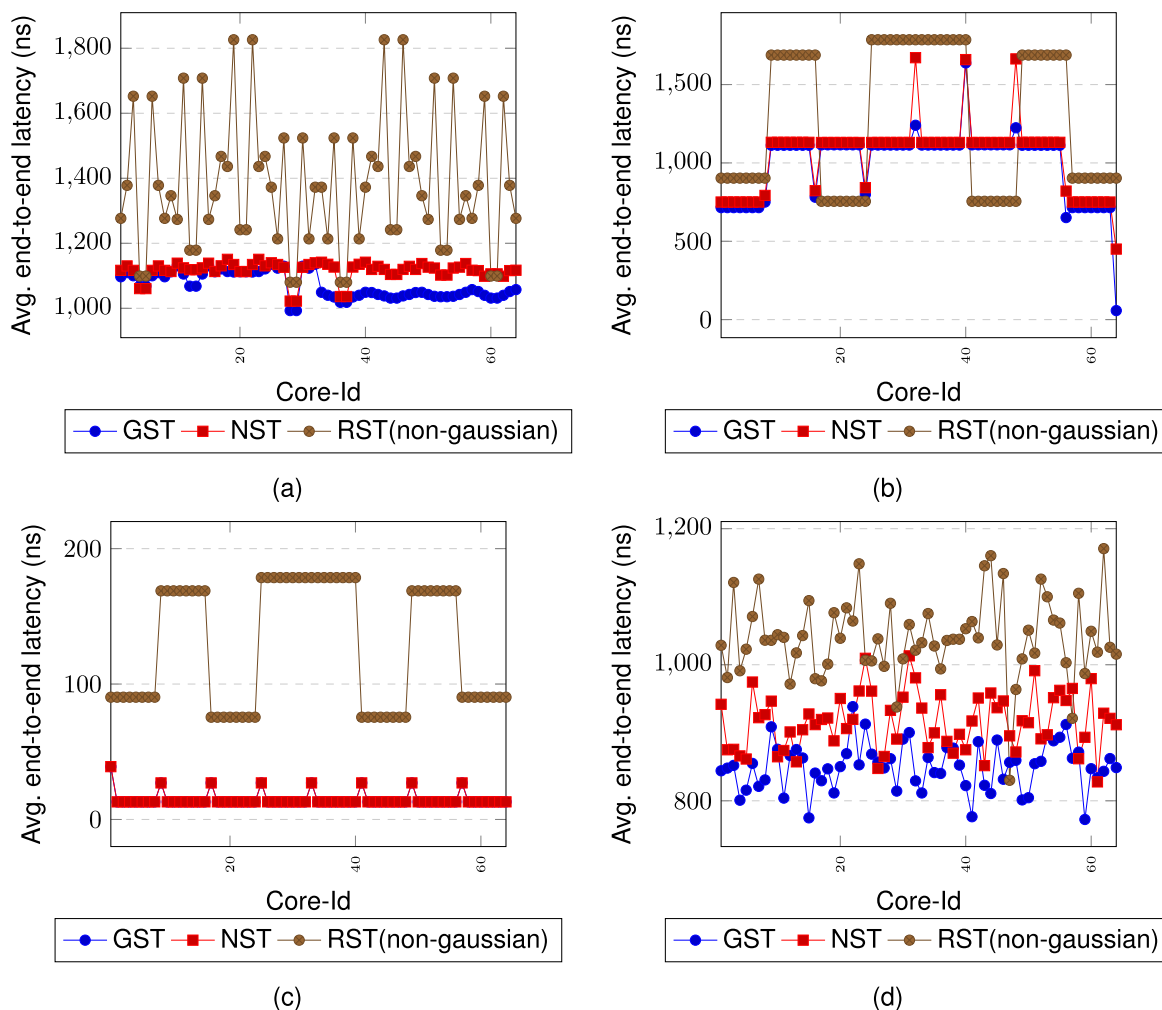


FIGURE 9. End-to-End Average Latency (ns) for 8 × 8 Mesh network topology for NGST, GST and RST process for traffic (a) Complement (b) Tornado (c) Neighbour (d) Uniform.

TABLE 2. OMNet++ Simulation Parameters.

Parameters	Simulation Value
Simulation duration	2μs
Flits per VC	1
Start time	1ns
Message Length	4 pkts
Flit Size	4 bytes
Flit arrival delay	2ns
No. of Virtual Channel (VC)	2
Arbitration	false
Packet Length	8 flits
Routing	XY routing

NGST, & RST processes are shown in TABLES 3 and 4 simulated parameters for the complement, tornado, uniform, and neighbour traffic.

TABLE 3. Average Packet-loss probability for 8 × 8.

Methods	Complement Traffic	Tornado Traffic	Uniform Traffic	Neighbour Traffic
Non-Gaussian	0.470	0.368	0.525	0.478
Gaussian	0.305	0.338	0.335	0.334
Rosenblatt	0.874	0.857	0.842	0.857

The traffic created by the Rosenblatt process is 11.87 % for uniform, 19.12 % for the complement, 18.85 % of the tornado, and 88.38 % for neighbour traffic bustier than NGST, as shown in TABLE 4. When compared to GST, complement receives 22.33 %, tornado receives 22.14 %, uniform receives 18.20 %, and neighbour traffic burstier receives 88.37 %. When compared to non-Gaussian, the produced Rosenblatt process is 56.96 % for the tornado, 46.22 % for the complement, 37.61 % for uniform, and 44.21 % for neighbour is more susceptible to losing packets from the buffer, whereas

TABLE 4. Average latency [ns] for 8 × 8.

Methods	Complement Traffic	Tornado Traffic	Uniform Traffic	Neighbour Traffic
Rosenblatt	1379.7	1283.1	1039.7	1283.9
Gaussian	1071.2	999.2	850.4	14.9
Non-Gaussian	1116.0	1042.6	916.3	14.9

in Gaussian is more susceptible to packet-loss, at 69.12 % for complement. For the power calculation, we used ORION3.0 [45] simulator where we used a uniform traffic pattern with an average power of 0.71 mW for the Rosenblatt process and 0.79 mW for the basic Hermite process, a difference of 11.29 %.

The Water Simulation with Spatial data structure, Hierarchical Radiosity, Barnes-Hut, Ocean Simulation, FFT, Blocked Sparse Cholesky Factorization and Radix Sort are used to compare the latency and power in FIGURE 8. For the SPLASH benchmark, the synthetic traffic corresponding to the RST has higher latencies and more power consuming than the synthetic traffic corresponding to the GST and the NST. The power evaluation is done based on the models of ORION3 [45]. It consists of libraries for the leakage and dynamic power based on the frequency of simulation for the 45nm and 65nm processes. The comparison of GST traffic with RST shows an improvement of 7.65% for normalized power consumption. The GST traffic excels over the RST in terms of power usage and the NGST process excels over the RST process by 11.56%.

The results indicate that RST-based traffic is more data-driven and more like represent real-time traffic which includes gaming traffics, high-definition video traffics, and other high-processing data streams whose packet arrival time cannot be perfectly predicted by a Gaussian-based traffic distribution.

Non-Gaussian processes are thus required for traffic modelling to reflect the optimized prediction of the network resources distributed within the multicore architecture. It will help network designers choose the right router queues, virtual channels, or arbitrators for their network. A buffer overflow, process cycle loss, significant energy dissipation, and network conflict might all occur from the wrong selection and quantity of these network resources.

V. CONCLUSION

The task of the network designer to choose the optimal network resources used in multicore communication is critical in the age of multi-core computing. We have been working towards the design of synthetic traffic, which is non-Gaussian in nature. We have used the benchmark suite to compare GST, NGST, and RST processes in terms of latency and power. We have compared the RST traffic under different traffic patterns for the mesh architecture. In all the cases the RST process shows higher power dissipation and latencies, shows the nature of higher order of burstiness in the traffic as

compared to NGST and GST traffic. We have compared the results with network latency, power dissipation, and packet-loss probability, and we found the Synthetic traffic, based on Rosenblatt process, compared to the Gaussian and regular non-Gaussian, is heavily burstier and more productive in predicting optimal network-resource selection for the network designers. The approach used to generate non-gaussian synthetic traffic opens new dimensions in the research of traffic modelling based on the time frame-based models. These models will have an impact on the deep-learning based algorithms for the generation of synthetic traffic using the forecasting methods on univariate data. In the future predictive machine learning models are used to generate the synthetic traffic and in estimating the exponential factor for representing long-tailed dependent traffic in order to support the bustier traffics.

REFERENCES

- [1] A. Valuskar, M. Shandilya, and A. Rajawat, "Statistical traffic pattern for mixed torus topology and pathfinder based traffic and thermal aware routing protocol on NoC," *Integration*, vol. 87, pp. 158–168, Nov. 2022.
- [2] R. Manju, A. Das, J. Jose, and P. Mishra, "SECTAR: Secure NoC using Trojan aware routing," in *Proc. IEEE/ACM Int. Symp. Netw.-on-Chip (NOCS)*, Sep. 2020, pp. 1–8.
- [3] A. Chronopoulou, F. G. Viens, and C. A. Tudor, "Variations and Hurst index estimation for a Rosenblatt process using longer filters," *Electron. J. Statist.*, vol. 3, pp. 1393–1435, Jan. 2009. Accessed: Nov. 17, 2022. [Online]. Available: <https://projecteuclid.org/journals/electronic-journal-of-statistics/volume-3/issue-none/Variations-and-Hurst-index-estimation-for-a-Rosenblatt-process-using/10.1214/09-EJS423.full>
- [4] K. S. Lii, M. Rosenblatt, and C. V. Atta, "Bispectral measurements in turbulence," *J. Fluid Mech.*, vol. 77, no. 1, pp. 45–62, Sep. 1976.
- [5] A. Fauth and C. A. Tudor, "Multifractal random walk driven by a Hermite process," in *Handbook of High-Frequency Trading and Modeling in Finance*, vol. 9. Hoboken, NJ, USA: Wiley, 2016, p. 221.
- [6] S. T. Rachev, S. Mittnik, and F. J. Fabozzi, "Pricing derivatives in Hermite markets," 2016, *arXiv:1612.07016*.
- [7] S. Torres and C. A. Tudor, "Donsker type theorem for the Rosenblatt process and a binary market model," *Stochastic Anal. Appl.*, vol. 27, no. 3, pp. 555–573, Apr. 2009.
- [8] I. Nourdin and T. T. D. Tran, "Statistical inference for Vasicek-type model driven by Hermite processes," *Stochastic Processes their Appl.*, vol. 129, no. 10, pp. 3774–3791, Oct. 2019.
- [9] C. Lévy-Leduc, H. Boistard, E. Moulines, M. S. Taqqu, and V. A. Reisen, "Asymptotic properties of U-processes under long-range dependence," *Ann. Statist.*, vol. 39, no. 3, pp. 1399–1426, Jun. 2011.
- [10] A. Chaurasia, "Performance of synthetic Rosenblatt process under multicore architecture," in *Proc. 3rd Int. Conf. Electron., Commun. Aerosp. Technol. (ICECA)*, Jun. 2019, pp. 377–381.
- [11] G. V. Varatkar and R. Marculescu, "On-chip traffic modeling and synthesis for MPEG-2 video applications," *IEEE Trans. Very Large Scale Integr. (VLSI) Syst.*, vol. 12, no. 1, pp. 108–119, Jan. 2004.
- [12] J. Barunik and L. Kristoufek, "On Hurst exponent estimation under heavy-tailed distributions," *Phys. A, Stat. Mech. Appl.*, vol. 389, no. 18, pp. 3844–3855, 2010.
- [13] G. Samorodnitsky, "Long range dependence," *Found. Trends Stochastic Syst.*, vol. 1, no. 3, pp. 163–257, 2007.
- [14] H. Fei and W. Zhimei, "Multifractal analysis and model of the MPEG-4 video traffic," in *Proc. IEEE Int. Perform., Comput., Commun. Conf.*, Apr. 2003, pp. 463–467.
- [15] S. Ma and C. Ji, "Modeling heterogeneous network traffic in wavelet domain," *IEEE/ACM Trans. Netw.*, vol. 9, no. 5, pp. 634–649, Oct. 2001.
- [16] Z. Qian, P. Bogdan, C.-Y. Tsui, and R. Marculescu, "Performance evaluation of NoC-based multicore systems: From traffic analysis to NoC latency modeling," *ACM Trans. Design Autom. Electron. Syst.*, vol. 21, no. 3, pp. 1–38, Jul. 2016.
- [17] P. Bogdan, "Mathematical modeling and control of multifractal workloads for data-center-on-a-chip optimization," in *Proc. 9th Int. Symp. Netw.-on-Chip*, Sep. 2015, pp. 1–8.

- [18] B. B. Mandelbrot and B. B. Mandelbrot, *The Fractal Geometry of Nature*, vol. 1. New York, NY, USA: Freeman, 1982.
- [19] W. H. Tranter, D. P. Taylor, R. E. Ziemer, N. F. Maxemchuk, and J. W. Mark, "On the self-similar nature of Ethernet traffic (extended version)," in *The Best of the Best: Fifty Years of Communications and Networking Research*. Hoboken, NJ, USA: Wiley, 2007, pp. 517–531.
- [20] V. Paxson and S. Floyd, "Wide area traffic: The failure of Poisson modeling," *IEEE/ACM Trans. Netw.*, vol. 3, no. 3, pp. 226–244, Jun. 1995.
- [21] R. G. Clegg, C. Di Cairano-Gilfedder, and S. Zhou, "A critical look at power law modelling of the internet," *Comput. Commun.*, vol. 33, no. 3, pp. 259–268, Feb. 2010. [Online]. Available: <https://www.sciencedirect.com/science/article/pii/S0140366409002540>
- [22] H. E. Hurst, "Long-term storage capacity of reservoirs," *Trans. Amer. Soc. Civil Eng.*, vol. 116, no. 1, pp. 770–799, Jan. 1951.
- [23] F. Vahdatpanah, M. Elahi, S. Kashi, E. Taheri, and A. Patooghy, "3DEP: A efficient routing algorithm to evenly distribute traffic over 3D network-on-chips," in *Proc. 27th Euromicro Int. Conf. Parallel, Distrib. Netw.-Based Process. (PDP)*, Feb. 2019, pp. 237–241.
- [24] G. Seetharaman and D. Pati, "Reliable fault-tolerance routing technique for network-on-chip interconnect," in *Intelligent Sustainable Systems*. Springer, 2022, pp. 767–775.
- [25] A. Gogoi, B. Ghoshal, A. Sachan, R. Kumar, and K. Manna, "Application driven routing for mesh based network-on-chip architectures," *Integration*, vol. 84, pp. 26–36, May 2022. [Online]. Available: <https://www.sciencedirect.com/science/article/pii/S0167926021001346>
- [26] R. Somisetty, V. S. S. Karthik, M. R. S. Srujan, and M. Vinodhini, "Congestion aware negative first routing with fair arbitration for network on chip," in *Proc. 6th Int. Conf. Comput. Methodol. Commun. (ICCMC)*, Mar. 2022, pp. 215–220.
- [27] N. Jindal, S. Gupta, D. P. Ravipati, P. R. Panda, and S. R. Sarangi, "Enhancing network-on-chip performance by reusing trace buffers," *IEEE Trans. Comput.-Aided Design Integr. Circuits Syst.*, vol. 39, no. 4, pp. 922–935, Apr. 2020.
- [28] S. Das, C. Karfa, and S. Biswas, "Formal modeling of network-on-chip using CFMS and its application in detecting deadlock," *IEEE Trans. Very Large Scale Integr. (VLSI) Syst.*, vol. 28, no. 4, pp. 1016–1029, Apr. 2020.
- [29] S. K. Mandal, R. Ayoub, M. Kishinevsky, M. M. Islam, and U. Y. Ogras, "Analytical performance modeling of NoCs under priority arbitration and bursty traffic," *IEEE Embedded Syst. Lett.*, vol. 13, no. 3, pp. 98–101, Sep. 2021.
- [30] M. Dlask, J. Kukal, and O. Vysata, "Bayesian approach to Hurst exponent estimation," *Methodol. Comput. Appl. Probab.*, vol. 19, no. 3, pp. 973–983, Sep. 2017.
- [31] G. Samorodnitsky, M. S. Taqqu, and R. W. Linde, "Stable non-gaussian random processes: Stochastic models with infinite variance," *Bull. London Math. Soc.*, vol. 28, no. 134, pp. 554–555, 1996.
- [32] M. Rosenblatt, "Independence and dependence," in *Proc. 4th Berkeley Symp. Math. Statist. Probab.*, vol. 2, 1961, pp. 431–443.
- [33] C. Tudor, *Analysis of Variations for Self-Similar Processes: A Stochastic Calculus Approach*. Cham, Switzerland: Springer, 2013.
- [34] M. Clausel, F. Roueff, M. S. Taqqu, and C. Tudor, "Wavelet estimation of the long memory parameter for Hermite polynomial of Gaussian processes," *ESAIM, Probab. Statist.*, vol. 18, pp. 42–76, Nov. 2014.
- [35] S. K. Mandal, A. Krishnakumar, and U. Y. Ogras, "Energy-efficient networks-on-chip architectures: Design and run-time optimization," in *Network-on-Chip Security and Privacy*. Berlin, Germany: Springer, 2021, pp. 55–75.
- [36] V. Adusumilli and V. Tg, "Traffic characterization based stochastic modelling of network-on-chip," *IEEE Trans. Comput.*, vol. 72, no. 4, pp. 1215–1222, Apr. 2023.
- [37] A. V. Bhaskar and T. G. Venkatesh, "Performance analysis of network-on-chip in many-core processors," *J. Parallel Distrib. Comput.*, vol. 147, pp. 196–208, Jan. 2021.
- [38] A. Chaurasia and V. K. Sehgal, "Performance of Gaussian and non-Gaussian synthetic traffic on networks-on-chip," *Int. J. Multimedia Data Eng. Manage.*, vol. 8, no. 2, pp. 33–42, Apr. 2017.
- [39] V. Pipiras, "Wavelet-based simulation of fractional Brownian motion revisited," *Appl. Comput. Harmon. Anal.*, vol. 19, no. 1, pp. 49–60, Jul. 2005.
- [40] R. A. Davis, K.-S. Lii, and D. N. Politis, "The Rosenblatt process," in *Selected Works of Murray Rosenblatt*. Berlin, Germany: Springer, 2011, pp. 29–45, doi: [10.1007/978-1-4419-8339-8_6](https://doi.org/10.1007/978-1-4419-8339-8_6).
- [41] I. Daubechies, *Ten Lectures on Wavelets*, vol. 61. Philadelphia, PA, USA: SIAM, 1992.
- [42] A. Chaurasia and V. K. Sehgal, "The MPEG-4 based energy efficient application traffic modelling and synthesis for network-on-chip architecture," *Sustain. Comput., Informat. Syst.*, vol. 23, pp. 67–79, Sep. 2019.

- [43] A. Varga, "OMNeT++," in *Modeling and Tools for Network Simulation*. Berlin, Germany: Springer, 2010, pp. 35–59, doi: [10.1109/LES.2015.2402197](https://doi.org/10.1109/LES.2015.2402197).
- [44] SPLASH-2. Accessed: Nov. 8, 2019. [Online]. Available: <http://www-flash.stanford.edu/apps/SPLASH/>
- [45] A. B. Kahng, B. Lin, and S. Nath, "ORION3.0: A comprehensive NoC router estimation tool," *IEEE Embedded Syst. Lett.*, vol. 7, no. 2, pp. 41–45, Jun. 2015.



AMIT CHAURASIA (Member, IEEE) received the B.Tech. degree in information technology from Uttar Pradesh Technical University, Lucknow, the M.Tech. degree in computer science from the Dayalbagh Educational Institute, Agra, in 2012, and the Ph.D. degree in computer science and engineering from the Jaypee University of Information Technology, Wakanaghat, Solan, Himachal Pradesh, India, in 2020. Since 2021, he has been an Assistant Professor with the Computer and Communication Engineering Department, Manipal University Jaipur, Jaipur, Rajasthan. He is the author of 11 articles. His research interests include synthetic traffic modeling for networks-on-chip, integration of knowledge graphs with blockchain, and consensus algorithm.



VIJAY SHANKAR SHARMA (Member, IEEE) received the B.E., M.E., and Ph.D. degrees from the MBM Engineering College, Jodhpur, which is one of the oldest engineering colleges in India. He is currently an Assistant Professor (senior scale) with the Department of Computer and Communication Engineering, Manipal University Jaipur, India. He has teaching experience of more than ten years. He has published 11 research papers in international and national journals/conferences. His research interests include networking and simulation, AI, ML, big data analytics, Hadoop, and the theory of computation.



CHIRANJIL LAL CHOWDHARY has been with the School of Information Technology and Engineering, Vellore Institute of Technology, since 2010, where he is currently an Associate Professor. His research interests include computer vision and image processing.



SHAKILA BASHEER is currently an Assistant Professor with the Department of Information Systems, College of Computer and Information Science, Princess Nourah bint Abdulrahman University, Saudi Arabia. She is working on Data Mining, Vehicular Networks Machine Learning, Block Chain, Vehicular Networks, and the IoT. She has more than ten years of teaching experience. She has worked and contributed in the field of Data Mining, Image Processing and Fuzzy Logic. She has published more technical papers in international journals/proceedings of international conferences/edited chapters of reputed publications. Her research also focuses on data mining algorithms using fuzzy logic.



THIPPA REDDY GADEKALLU (Senior Member, IEEE) is currently with Zhongda Group as a Chief Engineer and the School of Information Technology and Engineering, Vellore Institute of Technology, Vellore, India, as well as with the Department of Electrical and Computer Engineering, Lebanese American University, Byblos, Lebanon.